Acta Biomaterialia 89 (2019) 180–192

Contents lists available at ScienceDirect

Acta Biomaterialia

journal homepage: www.elsevier.com/locate/actabiomat

Full length article

Cardiomyocytes facing fibrotic conditions re-express extracellular matrix transcripts

Carlos O. Heras-Bautista [a,1], Nelly Mikhael [a,b,c,1], Jennifer Lam [a], Vaibhav Shinde [a], Alisa Katsen-Globa [d], Sabine Dieluweit [e], Marek Molcanyi [a], Vladimir Uvarov [g], Peter Jütten [g], Raja G.A. Sahito [a], Francisco Mederos-Henry [f], Alexander Piechot [g], Konrad Brockmeier [b], Jürgen Hescheler [a], Agapios Sachinidis [a,h], Kurt Pfannkuche [a,b,*]

[a] Institute of Neurophysiology, University of Cologne, Cologne, Germany
[b] Department of Pediatric Cardiology, University Hospital Cologne, Cologne, Germany
[c] Department of Clinical and Chemical Pathology, Cairo University, Cairo, Egypt
[d] Department of Biomedical Microsystems, Fraunhofer Institute for Biomedical Engineering, St. Ingbert, Germany
[e] Institute of Complex Systems, ICS-7: Biomechanics, Forschungszentrum Jülich GmbH, Jülich, Germany
[f] Institute of Condensed Matter and Nanosciences (IMCN), Division of Molecules, Solids and Reactivity (MOST), Université catholique de Louvain, Louvain-la-Neuve, Belgium
[g] Taros Chemicals GmbH & Co KG, Dortmund, Germany
[h] Center for Molecular Medicine Cologne, University of Cologne, Cologne, Germany

ARTICLE INFO

Article history:
Received 24 October 2018
Received in revised form 6 March 2019
Accepted 7 March 2019
Available online 9 March 2019

Keywords:
Fibrosis
Stem cells
Physiology
Biomarkers
Functional genomics
Heart remodeling

ABSTRACT

Pathophysiological conditions, such as myocardial infarction and mechanical overload affect the mammalian heart integrity, leading to a stiffened fibrotic tissue. With respect to the pathophysiology of cardiac fibrosis but also in the limelight of upcoming approaches of cardiac cell therapy it is of interest to decipher the interaction of cardiomyocytes with fibrotic matrix. Therefore, we designed a hydrogel-based model to engineer fibrotic tissue *in vitro* as an approach to predict the behavior of cardiomyocytes facing increased matrix rigidity. Here, we generated pure induced pluripotent stem cell-derived cardiomyocytes and cultured them on engineered polyacrylamide hydrogels matching the elasticities of healthy as well as fibrotic cardiac tissue. Only in cardiomyocytes cultured on matrices with fibrotic-like elasticity, transcriptional profiling revealed a substantial up-regulation of a whole panel of cardiac fibrosis-associated transcripts, including collagen I and III, decorin, lumican, and periostin. In addition, matrix metalloproteinases and their inhibitors, known to be essential in cardiac remodeling, were found to be elevated as well as insulin-like growth factor 2. Control experiments with primary cardiac fibroblasts were analyzed and did not show comparable behavior. In conclusion, we do not only present a snapshot on the transcriptomic fingerprint alterations in cardiomyocytes under pathological conditions but also provide a new reproducible approach to study the effects of fibrotic environments to various cell types.

Statement of Significance

The ageing population in many western countries is faced with an increasing burden of ageing-related diseases such as heart failure which is associated with cardiac fibrosis. A deeper understanding of the interaction of organotypic cells with altered extracellular matrix mechanical properties is of pivotal importance to understand the underlying mechanisms. Here, we present a strategy to combine hydrogel matrices with induced pluripotent stem cell derived cardiomyocytes to study the effect of matrix stiffening on these cells. Our findings suggest an active role of matrix stiffening on cardiomyocyte function and heart failure progression.

1. Introduction

The cardiac extracellular matrix (ECM) is a dynamic network of collagens, macromolecular proteoglycans, glycoproteins, proteases,

* Corresponding author at: Center of Physiology and Pathophysiology, Institute of Neurophysiology, University of Cologne, Medical Faculty, Robert-Koch-Str. 39, 50931 Cologne, Germany.
E-mail address: kurt.pfannkuche@uk-koeln.de (K. Pfannkuche).
[1] Both authors contributed equally.

https://doi.org/10.1016/j.actbio.2019.03.017
1742-7061/

growth factors and cytokines [1]. ECM facilitates mechanical, electrical and chemical signals during homeostasis and development as well as in mechanical stress whether physiological or pathological [2]. The healthy ECM is in a constant balanced state of protein synthesis and degradation which contributes to the needed heart tissue flexibility and compliance. However, during pathological mechanical stress (for e.g. pressure- and volume overload) or following myocardial infarction (MI), the myocardium undergoes complex structural remodelling with accumulation of ECM leading to a stiffened fibrotic matrix. The effect of passive myocardial stiffening is pronounced in pressure-overloaded tissue [3].

Most ECM proteins are produced by fibroblasts, including the main collagens I and III. However, in pathological conditions, myofibroblasts, neutrophils, mast cells and macrophages also contribute to ECM proteins synthesis (reviewed by Kong and colleagues [4]). Although cardiomyocytes are the most sensitive cells to the mechanical force changes occurring in the heart tissue [5], to date their role in the complex process of ECM synthesis, heart remodelling and fibrosis remains largely unexplored. Indeed, there are some hints, pointing to an increase in ECM production by cardiomyocytes under specific conditions. For example, Schram and colleagues found an increase in pro-collagen-I and -III expression in HL1 cardiomyocytes induced by leptin [6].

During remodeling, many genes that cease to be expressed in terminally mature cells are often re-expressed [7]. Nevertheless, generation of transcriptomic profiles from cardiomyocytes under pathophysiological conditions has proven to be a difficult task since generation of cell populations derived from fibrotic tissue biopsies is required. Firstly, it is essential to isolate pure cardiomyocytes; otherwise the observed alterations in gene transcription could also be attributed to other cell types of the heart. Secondly, only few viable cardiomyocytes survive the harsh isolation process. Finally and most importantly, cardiomyocytes face severe stress during their tissue isolation, which would most likely affect their transcriptome and inter-individual variations thus further limiting the significance of the data.

An alternative source of cardiomyocytes arises from the state-of-the-art stem cell technologies. Induced pluripotent stem (iPS) cells give rise to functional cardiomyocytes (iPS-CMs) *in vitro* and serve as a homogenous source of cardiomyocytes. It has been established that iPS-CMs show physiological response to adrenergic and cholinergic stimulation, express cardiac ion channels and develop contractile forces [8,9]. Antibiotics-driven lineage selection allows the generation of a pure population of cardiomyocytes devoid of contamination with undifferentiated cells [10] (Fig. 1).

Bioengineered polyacrylamide (PAA) based hydrogels with defined Young's moduli do not only form suitable substrates to culture iPS-CMs but can also sustain the culture for several weeks [11]. Tuning of hydrogel stiffness can be controlled through variation of acrylamide/bisacrylamide ratios prior to polymerization resulting in hydrogels that are optically clear and display linear elastic properties [12]. A previous study of our group has addressed the impact of conventional tissue culture plastics on the physiology of iPS-CMs and demonstrated deleterious effects of rigid substrates including sarcomere disassembly and loss of contractile ability [11]. On the contrary, iPS-CMs cultured on PAA hydrogels with a stiffness matching adult cardiac tissue remained functional for extended culture duration. In other words, cardiomyocytes optimal function and structure can only be preserved under physiological stiffness.

It has been long recognized that cardiomyocytes have the ability to sensitively respond to changes in the surrounding matrix elasticity [5,13–15]. A study by Panday and colleagues has recently demonstrated that spontaneously contracting cultured neonatal rat cardiomyocytes perform two types of contraction: rapid muscular contractions that result in the macroscopic shortening of the cells and slow non-muscular contractions that last for hours [16]. The slow non-muscular contractions are contributed to non-muscular myosin and occur only on the edges of cultivated cells. These slow contractions are crucial for cellular sensation of the matrix elasticity even during cyclic shortening of the tissue. Moreover, it was further shown that there is interplay between both forms of contraction resulting in variations of the degree of talin stretching depending on the matrix elasticity. These findings explain how cardiomyocytes gain information on the static mechanical feature of the surrounding matrix and provide further insights into the pathophysiology of cardiac fibrosis. Besides providing a platform to further investigate research questions related to endogenous cardiomyocytes in fibrotic stiffness, pluripotent stem cell-derived cardiomyocytes (PSC-CMs) have been considered as therapeutic agents replacing damaged fibrotic cardiac tissue. Recent studies in large animal models have proven the efficacy of such stem cell therapies [17,18]. However, safety concerns are remaining. Beside a high risk of arrhythmia initiation the long-term effects of transplanted PSC-CMs is not analyzed yet and the interaction of transplanted PSC-CMs with fibrotic cardiac tissue in an infarct patient remains to be studied.

In order to identify a potential role for cardiomyocytes during heart remodeling and maladaptive ECM production as well as to unravel the impact of fibrotic matrix stiffness on cardiomyocytes, we generated 123 kPa stiff PAA hydrogels [12] that comply with fibrotic myocardium stiffness *in vivo* [3,19,20]. For comparison, PAA hydrogels with the stiffness of embryonic cardiac tissue (12 kPa) and adult cardiac tissue (30 kPa) [21] were generated. iPS-CMs grown on conventional polystyrene substrates as a model for nearly infinite stiffness were included in the study [15].

2. Materials and methods

2.1. Preparation of hydrogel matrices

PAA hydrogels were prepared from sterile solutions of acrylamide (40% w/v) and bis-acrylamide (2% w/v) (both Bio-Rad Laboratories, Munich, Germany) using final concentrations of acrylamide and bis-acrylamide as follows 15% and 1.2% for stiff, 15% and 0.3% for medium, 8% and 0.2% for soft hydrogels. Solutions were buffered in 1.5 M sodium dihydrogen phosphate to a pH between 6 and 7.5 (NaH_2PO_4, Sigma-Aldrich, Taufkirchen, Germany). All solutions were degassed under vacuum for 15 min prior to polymerization. In order to generate the surface coating, the reactive crosslinking agent (2,5-Dioxopyrrolidin-1-yl) 6-(prop-2-enoylamino)hexanoate (DAH) (Stock was kept at −20 °C, each time aliquots were taken, the stock was left at RT for 15 min to prevent formation of condensed water) was co-polymerized and used to covalently bind fibronectin to the PAA hydrogel surface. DAH was provided by Taros Chemicals (Dortmund, Germany, see detailed synthesis protocol in the next paragraph) or synthesized as described [11]. DAH (6 mMol) was then added and samples briefly sonicated using an ultrasonic bath until DAH was completely dissolved. Polymerization was initiated by addition of 12.5 ul/ml of tetramethylethylenediamine (TEMED) diluted 1:10 in ultra-pure water and 12.5 μl/ml of freshly prepared ammonium persulfate (APS) (200 mmol in ultra-pure water) to the solution. Polyacrylamide support films were used (GelBond® Film, Lonza) as support. Sheets were cut using a punch tool to 3.5 cm. Polymerization was performed into the GelBond sheets (450 ul of polyacrylamide-DAH solution per Gelbond sheet) in closed Teflon casts to fabricate PAA gels with approximately 1 mm thickness (determined on the basis of the dimension of the mold). The resulting construct consisted of a support film, polyacrylamide hydrogel and DAH covalently bound to the surface of the hydrogel. After polymerization, PAA

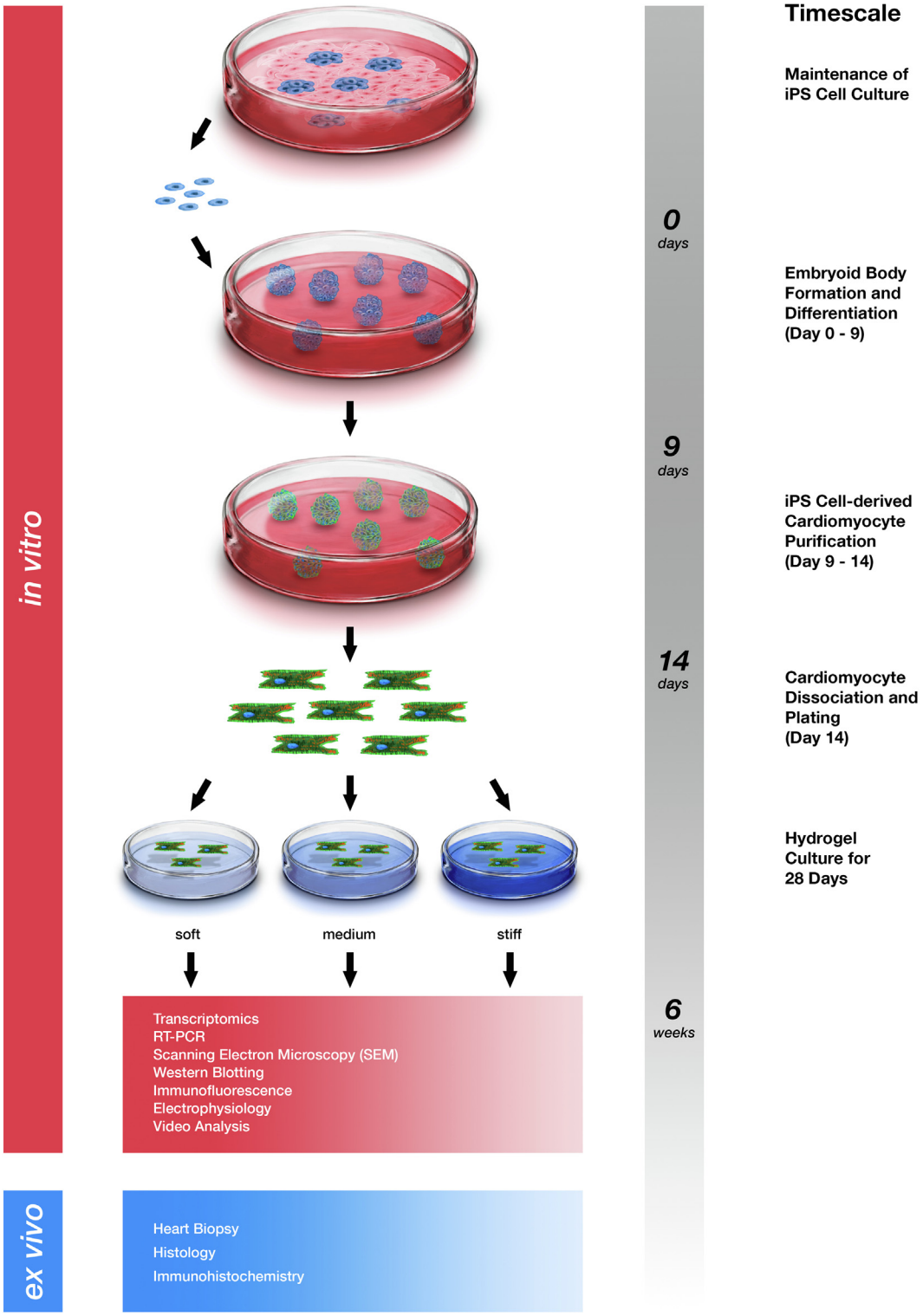

Fig. 1. Schematic illustration of the concept. Induced pluripotent stem (iPS) cells are maintained in culture and serve as a resource of cardiomyocytes for *in vitro* experiments. A transgene expressing puromycin-acetyltransferase under the control of a cardiac-specific promoter allows lineage selection of pure cardiomyocytes by puromycin. Purified cardiomyocytes are transferred to polyacrylamide hydrogels with variable stiffness in order to mimic physiological as well as pathophysiological (fibrotic) tissue elasticities. Cells are cultured on hydrogels for four weeks and collected for transcriptome analysis. Further experiments are designed on the basis of the transcription profile. Finally a prediction of transcriptional and physiological differences between cells in soft, medium and stiff matrix environments is constructed. Based on the prediction, working hypotheses are defined and can be validated using *in vivo* samples.

gels were washed twice with 50 mM *N*-2-hydroxyethylpiperazine-*N*-2-ethanesulfonic acid (HEPES), 7.4 pH. Next, 50 μl of 30 μg/ml bovine plasma fibronectin (Thermo Fisher Scientific, Germany) in HEPES (7.4 pH) was added to a petri dish coated with parafilm used as a hydrophobic interface, each active hydrogel was placed with the active side facing the protein solution and incubated for four hours at 4 °C. After the incubation period, fibronectin coated PAA gels were genlty detached from the parafilm and washed once with

HEPES (7.4 pH) and incubated with Iscovés modified Dulbeccós Medium (IMDM) for 2 h at 37 °C before cell seeding. Polystyrene dishes that were used as a control group were coated overnight with fibronectin (2.5 μg/ml).

2.2. Synthesis of DAH

Analytical HPLC and Electron Spray Ionization (ESI) mass spectra were performed on a Waters HPLC (2525 Binary Gradient Module, Milford, MA, USA) equipped with a Diode Array Detector and a Quadrupole MS using mixture gradients of acetonitrile/water/formic acid as solvents using C18 column (XBridge C18 5 μm, 4.6x100 mm). ^{1}H NMR spectra were recorded at ambient temperature using a Bruker Avance II 300 spectrometer (Bruker BioSpin, Fällanden, Switzerland).

2.3. Step 1: Synthesis of 6-Acrylamidohexanoic acid

6-Aminohexanoic acid (14.5 g, 110 mmol) was dissolved in a solution of sodium hydroxide (11.0 g, 276 mmol) in water (75 mL). The mixture was cooled to 5 °C in an ice bath, and a solution of acryloyl chloride (11.9 g, 132 mmol) in dichloromethane (75 mL) was added dropwise over a period of 1 h. Then 10% aqueous hydrochloric acid was added to adjust the pH of the reaction mixture to 3. The precipitate was filtered off, washed with water (150 mL) and dried in high vacuum. The product was recrystallized from ethyl acetate to afford the title compound as a white solid (14.9 g, 73%). ^{1}H NMR (CD_3OD, 300 MHz) δ = 6.28 (dd, 1 H, ^2J 1.5 Hz, ^3J 17.0 Hz, C*H*H'=CH), 6.11 (dd, 1 H, ^3J 17.0 & 10.2 Hz, CHH'=C*H*-), 5.92 (br t, 1 H, N*H*), 5.53 (dd, 1 H, ^2J 1.5 Hz, ^3J 10.2 Hz, CH*H*'=CH), 3.35 (m, 2 H, H-*6*), 2.36 (t, 2 H, ^3J 7.3 Hz, H-*2*), 1.67 (m, 2 H, H-*5*), 1.57 (m, 2 H, H-*3*), 1.40 (m, 2 H, H-*4*). ESI-MS: *m*/*z* calcd for $C_9H_{15}NO_3$: 185. Found: $[M + H]^+$ 186, $[M + Na]^+$ 208, [Na salt + Na]$^+$ 230.

2.4. Step 2: Synthesis of DAH from 6-Acrylamidohexanoic acid

6-Acrylamidohexanoic acid (14.90 g, 80 mmol) and *N*-hydroxysuccinimide (9.25 g, 80 mmol) were suspended in dry CH_2Cl_2 (215 mL). 1-Ethyl-3-(3-dimethylaminopropyl)carbodiimide (18.40 g, 96 mmol) was then added in one portion under cooling with ice. The reaction mixture was stirred at room temperature overnight when LC-MS indicated complete consumption of the starting material. After cooling to 5 °C, acetic acid (0.2 mL) was added and the mixture stirred for 10 min. The cold mixture was washed with ice cold saturated aqueous sodium bicarbonate (2x150 mL), cold brine (100 mL) and dried ($MgSO_4$). Concentration of the organic solution afforded a white solid (20.36 g, 90%). ^{1}H NMR ($CDCl_3$, 300 MHz). δ = 6.28 (dd, 1 H, ^2J 1.7 Hz, ^3J 17.0 Hz, C*H*H'=CH), 6.11 (dd, 1 H, ^3J 17.0 & 10.1 Hz, CHH'=C*H*-), 5.92 (br t, 1 H, N*H*), 5.53 (dd, 1 H, ^2J 1.7 Hz, ^3J 10.1 Hz, CH*H*'=CH), 3.35 (m, 2 H, H-*6*), 2.84 (m, 4 H, COCH_2CH_2CO), 2.62 (t, 2 H, ^3J 7.1 Hz, H-*2*), 1.78 (m, 2 H, H-*5*), 1.56 (m, 2 H, H-*3*), 1.48 (m, 2 H, H-*4*). ESI-MS: *m*/*z* calcd for $C_{13}H_{18}N_2O_5$: 282. Found: $[M + H]^+$ 283, $[M + Na]^+$ 305, $[2 M + H]^+$ 565, $[M + Na]^+$ 587.

2.5. Estimation of Young's moduli by atomic force microscopy

AFM experiments were carried out using a commercial AFM, Nanowizard (JPK, Germany) that was operated in spectroscopy mode. The samples were measured in phosphate-buffered saline (PBS -/-) and he indentation was carried out at a velocity of 1 μm/s. Several points from each gel sample were measured to ensure homogeneity and each point was measured repeatedly. According to the expected stiffness of the sample, four different standard silicon or silicon nitride cantilevers were used with a nominal spring constant of k = 42 N/m (Atomic Force, Germany), k = 2.8 N/m (Nanoandmore, Germany), k = 0.58 N/m or k = 0.32 N/m (Veeco, Germany). Tips had a conical shape with an opening angle of 20°, 18° and 35° respective to the used cantilevers The actual spring constant was determined using thermal fluctuations in air [22]. The sensitivity was determined in PBS-/- on glass. AFM data were processed by JPK Software and the force indentation depth curves were fitted by extended Hertz model to obtain the elasticity [23–26].

2.6. Cell lines and cell culture

A single clone of the murine iPS cell line TaP4 was used for this study [27]. We choose this clone because it is used frequently in our laboratory and has been extensively characterized [27]. TαP4 gives rise to atrial-, nodal- and ventricular-like types of cardiomyocytes and show intact hormonal regulation. Furthermore, TαP4 was used in a previous study to analyse the effect of long-term culture of iPS-cell derived cardiomyocytes on polyacrylamide hydrogels and conventional cell culture plastics [11]. The cells carry a transgene expressing the puromycin-acetyltransferase under control of cardiac specific alpha myosin heavy chain promoter allowing antibotics-driven lineage selection of cardiomyocytes.

Stem cells were cultured on murine embryonic feeder (~20.000 cells/cm^2) cell layers grown on 0.1% gelatin coated dishes. Feeder cells were inactivated by mitomycin C (Serva, 10 μg/ml for 2–4 h) treatment. iPS cells were cultured in stem cell maintenance medium composed of IMDM supplemented with 17% fetal calf serum (FCS), 1% non-essential amino acids (100x supplement MEM), 100units/ml penicillin, 100 μg/ml streptomycin and 1000 units/ml leukemia inhibitory factor (ORF genetics, Reykjavik, Iceland). All reagents were purchased from Thermo Fisher Scientific if not stated otherwise. Differentiation was performed as described in detail before [28]. To initate differentiation, 10^6 undifferentiated iPS cells per 10 cm dish (bacteriological dish to prevent adhesion) were cultured in form of a single cell suspension on a rocking table at 80 revolutions per minute to form embryoid bodies (EBs). Medium was composed of IMDM + Glutamax with 20% FCS, non-essential amino acids (1x, Thermo Fisher Scientific) and 200 μg/ml L-Ascorbic-Acid-Phosphate-Magnesium-Salt-n-Hydrate (Wako Chemicals, Neuss, Germany). On day 2 of differentiation EBs were diluted to about 800 EBs/10 cm dish in IMDM supplemented with 20% FCS, 1% non-essential amino acids and 50 μg/ml L-Ascorbic-Acid-Phosphate-Magnesium-Salt-n-Hydrate and further cultured under continuous agitation. On day 7 EBs were pooled (2 plates into 1 plate) and fresh medium (containing 5% FCS for the period of purification) was added. Beating cardiomyocytes appeared on day 8 of differentiation and cardiomyocytes selection was initiated by addition of 8 μg/ml puromycin (Gibco™ by Thermo Fisher Scientific). Medium was changed daily and puromycin was added until day 12. On day 12, EBs were collected in a 15 mL tube, and washed three times with phosphate buffered saline (Ca^{2+} and Mg^{2+} free) to remove any cell debris and serum. Trypsin (0.15%; 1:1 mixture of 0.05 and 0.025 trypsin; Gibco™ by Thermo Fisher Scientific) was added to the EBs. Incubation took place for 1–1,5h at room temperature. The supernatant was then collected in a 50 mL tube containing 5 mL FBS and EBs were treated with fresh trypsin (0.15%). After EBs had precipitated by gravity, supernatant was collected and added to the FBS mixture. This process was repeated until there was no immediate color change in trypsin when added to the EBs and EBs had decreased in size. EBs were then re-suspended to single CMs and added to the collection tube

which was centrifuged at 95*g* for 10 min. Supernatant was aspirated, the CM cell pellet was re-suspended in phosphate buffered saline and strained through a 40 μm mesh sieve. CMs were counted, centrifuged and plated (110,000 cells/cm^2) on fibronectin coated cell-culture plates without puromycin. The next day (day 13), CMs were washed with phosphate buffered saline to remove cell debris and cultured in puromycin-supplemented medium. Medium was changed daily until day 15.

2.7. Cardiomyocyte culture on hydrogels

For seeding of hydrogels puromycin-purified cardiomyocytes (day 15, see section above) were washed with Ca^{2+}/Mg^{2+}-free phosphate buffered saline, trypsinized (0.05%), strained and diluted (1x10^4 cells/μl) in culture medium (IMDM, supplemented with 5% FCS). For one well of a 6-well plate, 100 μl of CM-suspension (1x10^6 cells; ~110,000 cells/cm^2) was carefully distributed on the gel in a drop-wise manner. The following day, cells were washed and medium was switched to IMDM medium supplemented with 20% FCS. Cells were cultured at 37 °C and 5% CO_2 for up to 4 weeks. Medium was changed every other day.

2.8. Isolation of adult mouse cardiac fibroblasts

Murine cardiac fibroblasts (CFs) were isolated from the hearts of adult C57BL6 x SV192 F1-generation mice (>6 months old, n = 8). Three independent experiments were performed. Hearts were excised after cervical dislocation and thoracotomy and washed several times with calcium-free ice cold Krebs-Ringer saline. Ventricular tissue was dissected, washed and minced using small surgical scissors. Tissue pieces were predigested with 4 U/ml bacterial proteinase (Sigma Aldrich) for 15 min followed by 20 min of incubation in 1 mg/ml collagenase A and 0.5 mg/ml hyaluronidase at 37 °C with gentle agitation. Repeated cycles of digestion with 1.0 mg/ml collagenase A for 20 min each were performed until tissue was completely digested. Following each digestion cycle, the supernatant was collected, centrifuged at 600 rpm for four minutes and re-suspended in culture medium supplemented with 20% FCS. Cells were pooled and cultured on fibronectin-coated dishes for 2 h to allow for the preferential attachment of CFs. The supernatant was then replaced with fresh culture medium. After 24 h, the attached CFs were dissociated via trypsinization (0.05%) and cultured on soft, medium and stiff hydrogels as well as fibronectin-coated polystyrene dishes at a concentration of 2x10^{4}cells/cm^2 for 28 days. Medium was exchanged every two days.

2.9. Microarrays

Microarray analysis was performed as described previously [29]. Briefly, total RNA was isolated using TRIzol and chloroform (Sigma-Aldrich), purified with miRNeasy mini kit (Qiagen, Hilden, Germany), and quantified using NanoDrop (ND-1000, Thermo Fisher Scientific, Langenselbold, Germany). For microarray labelling, 100 ng total RNA isolated from cardiomyocytes was used as a starting material and after amplification 12.5 μg amplified RNA were hybridized on Mouse Genome 430 version 2.0 arrays (Affymetrix, Santa Clara, CA, USA) for 16 hrs at 45 °C. The arrays were washed and stained in Affymetrix Fluidics Station-450 according to the manufacturer's instructions. For fibroblasts analysis a new generation of microarrays (Clariom™ S arrays, Applied Biosystems by Thermo Fisher Scientific) was used. 5.5 μg fragmented biotin-labeled ds cDNA from cardiac fibroblasts were hybridized to Clariom™ S arrays. After staining, arrays were scanned with Affymetrix Gene-Chip Scanner-3000-7G while quality control analysis was performed using Affymetrix GCOS software.

2.10. Statistical data and functional annotation analysis

Statistical data analysis and visualization have been performed by uploading .cel files in Partek Genomics suite (PGS) version 6.6 (Partek, St Louis, MO, USA). The probe set intensity values were generated by RMA background correction, quantile normalization, log2 transformation and median polished probe set summarization. The normalized probe sets were used for the generation of principal component analysis (PCA) and one-way ANOVA model was used to generate the differentially regulated transcripts with at least a 2-fold change. The signals of differentially regulated transcripts were normalized by Z score and clustered using hierarchal cluster analysis (unsupervised, PGS). The commonly deregulated transcripts were acquired by generation of Venn diagrams (PGS). The online free software Database for Annotation, Visualisation and Integrated Discovery (DAVID) was used for functional annotation and gene ontology (GO) clustering of differentially expressed transcripts. Identification of cellular identity based on the transcription profile was done using the open access software tool Cellnet (http://pcahan1.github.io/cellnetr/) [30,31].

2.11. Real time PCR

Direct isolation of mRNA and subsequent cDNA synthesis was accomplished with the μMACS One-step cDNA Kit (Miltenyi Biotech, Bergisch Gladbach, Germany) according to the manufacturer's instructions. Using QuantiTect SYBR® Green Mastermix (Qiagen, Hilden, Germany) qPCR was performed on Applied Biosystems 7500. PCR reaction was initiated at 50 °C for 2 min, followed by 95 °C for 10 min and 40 cycles of 15sec at 95 °C and 1 min at 60 °C.

While GAPDH served as endogenous control (ΔCt), cells plated on PAA gel matrices with medium stiffness were used as calibrator (ΔΔCt). Primers used were: GAPDH-F: ggctcatgaccacagtccat; GAPDH-R: accttgcccacagccttg and QuantiTect Primer Assays (Qiagen): Fabp5 (QT00240226), Kcna1 (QT01537263), Col1a2 (QT01055572), Col3a1 (QT02331301) and Igf2 (QT00109879).

2.12. Immunocytochemistry

The cells were washed with PBS and fixed with 4% paraformaldehyde for 15 min. For the fibrotic human biopsy samples, probes were de-paraffinised and antigen retrieval performed by incubation with trypsin 0.25% for 30 min at 37 °C. Permeabilization was done using 0.2% Triton X100 in PBS-Tween for 20 min. 10% Roti-Immunoblock (T144.1, Carl Roth) was used to block non-specific protein-protein interactions for 1–2 h at room temperature. Primary antibodies used were as follows: the rabbit polyclonal anti-IGF2 antibody (ab9574, abcam) at a concentration of 1:500; mouse monoclonal anti-alpha-Actinin (Sarcomeric) antibody (clone EA-53, A7811, Sigma-Aldrich) 1:800. Specimens were incubated overnight at 4 °C. The secondary antibody Alexa Fluor 488 goat anti-rabbit IgG (H + L) (A11034, Invitrogen), and Alexa Fluor 555 goat anti-mouse IgG1 (A10538, Life Technologies) were used at a concentration of 1 μg/ml and incubated for 1 h at room temperature. Simultaneously, nuclei were stained with Hoechst 33342. Images were taken from randomly chosen fields using the Axiovert 200 fluorescence microscope and AxioVision 4.5 software. Alpha-actinin images were captured using an upright confocal microscope (TCS SP8 MP-OPO, Leica) and LAS AF 3 software at the imaging facility of CECAD institute (Cologne).

The mean cell fluorescence of Igf2 stainings was measured using the free software ImageJ after normalization to the background. Differences between groups were analyzed using One-way ANOVA with Kruskal-Wallis post-hoc test. Statistical analysis

was performed using Prism Graphpad software (version 5, San Diego, California, USA).

2.13. Scanning electron microscopy

For scanning electron microscopy (SEM) iPS-CMs cultivated on the PAA-hydrogel with different stiffness were washed in PBS and fixed with 2% glutaraldehyde on the 0.1 M cacodylate buffer. Then the cells were prepared for SEM as followed: post-fixed with 2% osmium tetroxide in cacodylate buffer, and treated with 1% tannic acid and 1% uranyl acetate in distillated water [31]. The samples were then dehydrated in increasing alcohol concentrations, dried in hexamethyldisilazane (HMDS, Sigma-Aldrich, Taufkirchen, Germany), and coated with carbon. All samples were studied in field emission scanning electron microscope Phillips FESEM XL30 (FEI, Eindhoven, Netherlands) using secondary electron (SE)-, and backscattered electron (BSE)-modes.

3. Results

3.1. Cardiomyocyte structure and function is disturbed on fibrotic-like stiffness substrate

In order to develop an *in vitro* system to study the pathophysiology of the fibrotic heart, we engineered cardiac tissue models using iPS-CMs seeded on elasticity controlled PAA gel matrices. PAA substrates reflecting the stiffness of embryonic (soft gel), adult (medium gel) and fibrotic (stiff gel) cardiac tissue were casted into Teflon molds as previously described by our group. Substrates were probed for their elastic properties by force spectroscopy with an atomic force microscope resulting in elasticities of 12 ± 3 kPa (soft gel, N = 3 (number of gels), n = 63 (number of indentations analyzed)) and 30 ± 4 kPa (medium gel, N = 6, n = 191). Stiff hydrogel probing resulted in 123 ± 21 kPa (N = 8, n = 232). Heterobifunctional crosslinker (DAH) was used to covalently link fibronectin to the substrate surface since fibronectin has been successfully used for long-term cultivation of murine iPS-CMs in a previous study [11]. Induced pluripotent stem cell-derived cardiomyocytes were generated from murine iPS cells strain TαP4 expressing puromycin acetyltransferase under control of the cardiomyocyte-specific alpha-myosin-heavy chain promoter [32]. Puromycin selection resulted in a population of pure iPS-CMs that can be used for long-term culture studies without the appearance of undifferentiated colonies as previously described [32].

Induced pluripotent stem cell-derived cardiomyocytes were cultured on soft, medium and stiff hydrogels as well as on polystyrene for a period of four weeks. iPS-CMs on soft and medium hydrogels formed monolayers of rhythmically contracting cells (video 1, and video 2). In contrast, iPS-CMs on stiff hydrogels displayed an arrhythmical beating behavior in most preparations (videos 3 and 4) characterized by short bouts of contraction followed by periods of inactivity. Among all used substrates, rigid plastic polystyrene performed worst and disturbed the contractile function of cultured iPS-CMs the most (video 5).

To analyze the sarcomere organization, purified iPS-CMs were stained with antibodies against the z-disc protein alpha-actinin. Analysis on an upright confocal microscope revealed highly organized sarcomere structures on soft and medium hydrogels (Fig. 2 and supplementary Fig. 1). The left panel of Fig. 2 gives an example of an iPS-CM on stiff gel with disarranged sarcomere structure as indicated by varying orientations of the z-disc throughout the individual cell. Moreover, α-actinin is found in fiber-like structures. For comparison the second panel shows a group of iPS-CMs on stiff gel with a higher degree of organization and no fiber-like α-actinin structures. Supplementary Fig. 1 shows iPS-CMs that were cultured for 2–3 weeks on medium and stiff hydrogels, further illustrating the appearance of disarranged sarcomeres in iPS-CMs on stiff hydrogels. Of note, sarcomere disruption could be identified in individual cells on medium gels (supplementary Fig. 1, red arrows).

3.2. Fibrotic- like stiffness exhibits the most significant deviation from a healthy transcriptome

To further advance our understanding about the effect of the fibrosis-like matrix on cardiomyocytes, RNA was isolated, hybridized to Affymetrix gene arrays and analyzed for differences in individual transcripts.

Hierarchical cluster analysis showed a strong similarity between iPS-CMs cultured on soft and medium hydrogels (supplementary Fig. 2). In contrast, the transcriptome of iPS-CMs cultured on conventional polystyrene substrates differed significantly from these two groups. However, the most variable expression was displayed by iPS-CMs on stiff hydrogels as compared to those on medium hydrogels representing physiological myocardial matrix stiffness and serving as a reference group. Unexpectedly, the expression profiles of iPS-CMs on stiff hydrogels and polystyrene did not converge at all.

Differentially-regulated transcripts were analyzed in comparison to iPS-CMs on medium hydrogels revealing an overlap of only few genes between the individual groups (Fig. 3A). iPS-CMs on soft hydrogels showed only ten specifically de-regulated transcripts as compared to medium hydrogels, both accounting for healthy embryonic and adult cardiac tissue respectively. On the other hand, on stiff hydrogels, 506 specifically up- and 365 specifically down-regulated genes were identified. On polystyrene, 233 specifically up- and 403 down-regulated transcripts were detected. Only 50 and 33 identical genes were up- and down-regulated on polystyrene and stiff hydrogel respectively. The whole set of 2-fold and higher de-regulated transcripts in all groups compared to medium hydrogels is summarized in Supplementary Table 1. The probe set of absolute values is provided in Supplementary Table 2.

Gene ontology (GO) analysis of deregulated transcripts was performed to identify biological processes affected by fibrosis-like stiffness (Supplementary Table 3). Analysis of the deregulated genes from iPS-CM that were cultured on polystyrene indicated up-regulation of transcripts involved in "stress response" (23 transcripts), "actin cytoskeleton organization" (9 transcripts) and "cell proliferation" (9 transcripts) while transcripts related to the GOs "programmed cell death" (21 transcripts), "heart development" (12 transcripts) and "regulation of cell cycle" (10 transcripts) were suppressed (Fig. 3B). Most strikingly, 141 genes related to metabolic processes were found to be down-regulated when iPS-CMs were grown on polystyrene. In summary, these data suggest an adaptation mechanism of iPS-CMs grown on conventional plastic surfaces, resulting in an increased resistance to stress and other major changes in the cellular metabolome.

On the other hand, iPS-CMs cultured on stiff hydrogels revealed increased expression of a high number of transcripts associated with "multicellular organismal development" (102 transcripts; $p = 5.4*10^{-14}$). Among them we identified genes associated with "nervous system development" (49 transcripts, $p = 2.3*10^{-11}$), "anatomical structure morphogenesis" (55 transcripts, $p = 2.8*10^{-10}$), "mesoderm development" (28 transcripts, $p = 5.6*10^{-6}$) and "ectoderm development" (31 transcripts, $p = 1.3*10^{-5}$). Genes belonging to the "cell cycle process" (21 transcripts, $p = 1.2*10^{-6}$) were found to be downregulated (Fig. 3C). The GO analysis indicated a massive induction of developmental programs in iPS-CMs grown on stiff hydrogels and led to the conclusion that the cells underwent a broad adaptation to matrix stiffening accompanied with structural re-organization. Fig. 3D compares the up- and downregulation of those transcripts that

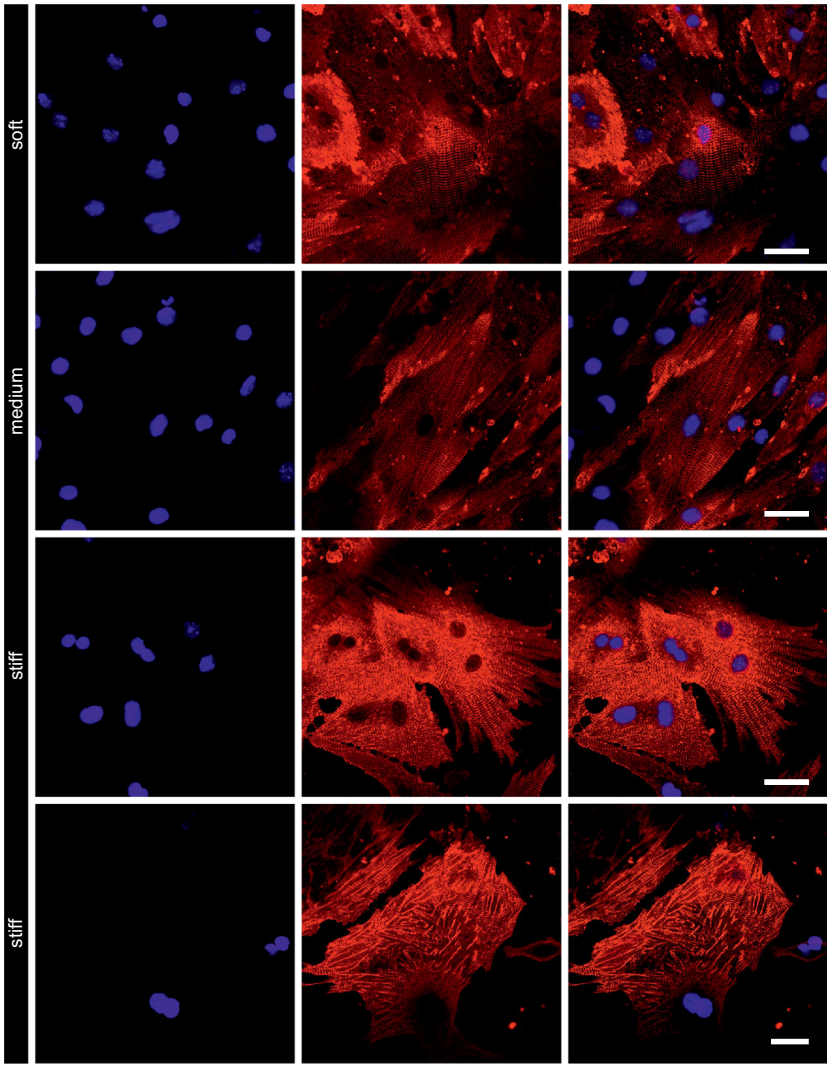

Fig. 2. Sarcomeric structure in iPS-CMs cultured on matrices with different elasticities. Purified iPS-CMs were transferred to polyacrylamide hydrogels with elasticities resembling embryonic (soft), adult (medium) or fibrotic (stiff) tissue and cultured for four weeks. Immunocytochemical staining of z-discs was performed with antibodies against sarcomeric alpha actinin (red). Nuclei were counterstained by Hoechst dye (blue). All images were acquired on an upright confocal microscope. Scale bar: 30 μm. (For interpretation of the references to color in this figure legend, the reader is referred to the web version of this article.)

show the highest upregulation in iPS-CMs on stiff gels as compared to medium gels graphically in form of a heatmap.

We did not observe growth of contaminating stem cell colonies in our cardiomyocyte cultures. However, to further exclude the possibility that a potential de-differentiation or occurring impurities in our cell preparation could have resulted in the expansion of non-cardiomyocytes, the complete transcriptomic data set was analyzed by the CellNet Software. The CellNet software linked our transcriptome data to known transcriptomes of various cell types [30]. The result is plotted as a heatmap and further confirms the absence of pluripotent transcription profiles and defines our cells as cardiomyocytes under all four culture conditions (supplementary Fig. 3). To give even more weight to this observation we analysed the expression data for transcripts specific for cardiomyocytes, pluripotent stem cell and proliferating cells. The result of this analysis is given in Table 1. The transcripts of the pluripotency specific markers "transcripts octamer binding factor 4" (Oct4, Pou5F1), "sex determining region Y box 2" (Sox2), and the cyclins A1 and B2 (Ccna1, CcnB1) show values in the range of background noise. In contrast, the cardiac specific transcripts cardiac troponin T (Tnnt2) and cardiac alpha actinin (Actc1) display high expression values in all samples.

3.3. Increased expression of ECM protein transcripts in iPS-CMs on fibrotic-like stiffness hydrogels

Recently, Qiu and colleagues have described an *in vitro* model based on polydimethylsiloxane (PDMS) matrices with a Young's modulus of 17.5 ± 4.2 kPa and 145.3 ± 18.0 kPa to study the effects of stiffened cardiac matrix on the physiology and expression profile of primary ovine and murine cardiac progenitor cells *ex vivo* [33]. The results by Qiu demonstrated variations in the expression of matrix proteins with strong increase in the expression of a set of collagen proteins (Col1a1, Col3a1, Col4a1, Col4a2, Col5a1and Col6a1) with Col3a1 showing the most prominent up-regulation (about 15-fold). Our data from pure iPS-CMs revealed an increased expression of several collagen proteins including Col1a1 (12.8-fold), Col1a2 (24.0-fold), Col5a2 (7.7 fold), Col6a3 (11.4-fold), and Col8a2 (4.4-fold) during culture on stiff hydrogels, with Col3a1 showing the highest up-regulation (54.3-fold).

iPS-CMs cultured on stiff hydrogels showed increased expression of matrix metalloproteinases (Mmp2, Mmp14) (5.4-fold, 3.4-fold respectively), tissue inhibitors of metalloproteinases 2 and 3 (Timp2, Timp3) (2.5-fold, 2.4-fold respectively), secreted phosphoprotein 1 (Spp1) (4.9-fold) and tenascin C (Tnc) (6.5-fold).

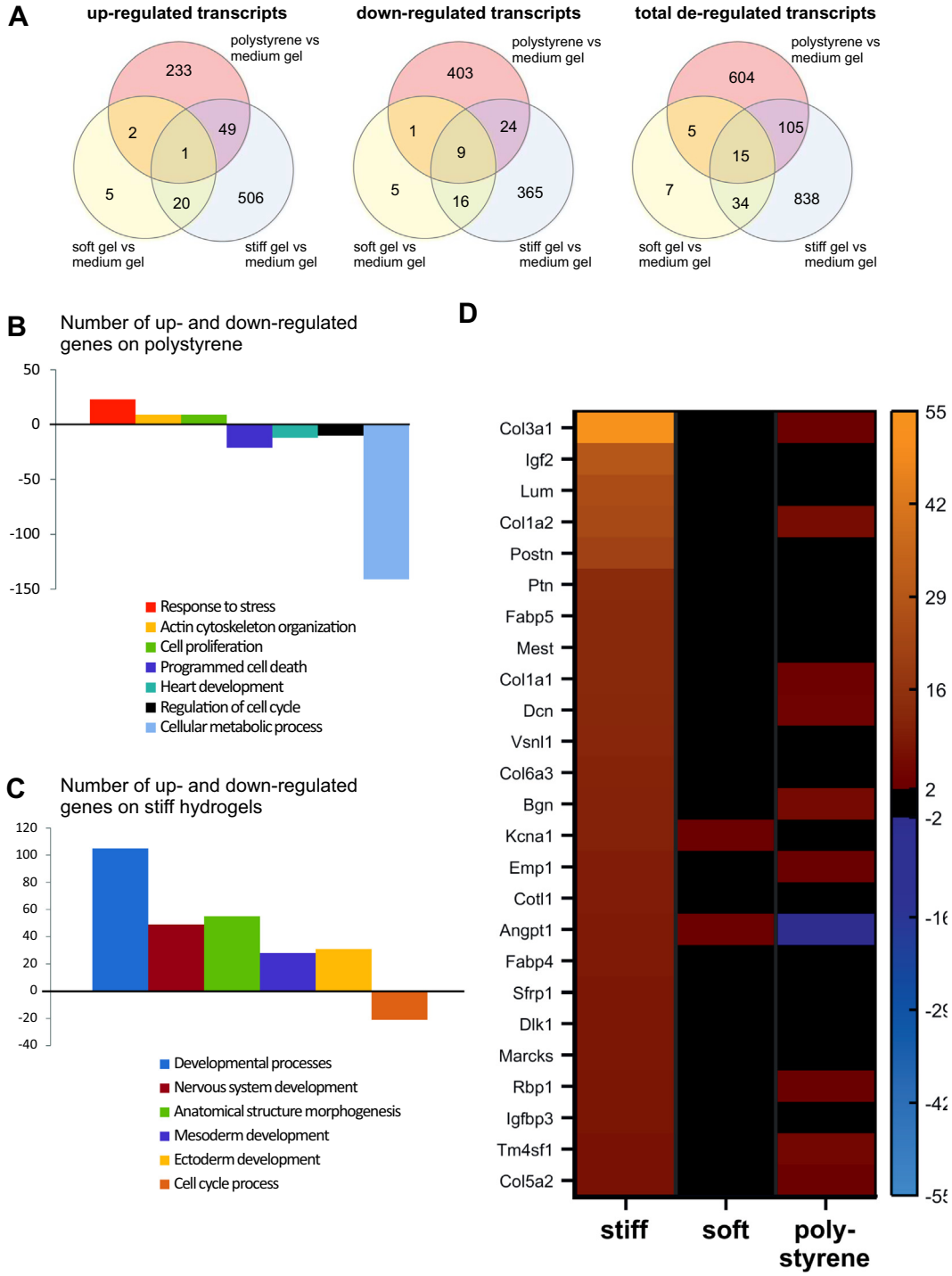

Fig. 3. Transcriptome analysis. Gene expression profiles of iPS-CMs grown for four weeks on soft, medium and stiff polyacrylamide hydrogels were acquired by gene array profiling. iPS-CMs grown on polystyrene cell culture dishes were included as a condition of near infinite stiffness. Differentially regulated transcripts (>2-fold) were compared to the transcription level in iPS-CMs grown on medium hydrogels. Numbers of up- and downregulated genes are shown in the Venn diagram (A). Gene ontology analysis was applied to identify affected pathways. Panel (B) and (C) display the numbers of transcripts that relate to the specified pathways. Top upregulated genes on stiff hydrogels are displayed in panel (D) in form of a heatmap in comparison to soft hydrogel and polystyrene (all groups were normalized to medium hydrogels).

In order to validate the gene expression profiles, five remarkably up-regulated transcripts in iPS-CMs on stiff gels were chosen, i.e. Fabp5, Igf2, Kcna1, Col1A2, and Col3A1. RNA was isolated from samples independent of those generated for gene array profiling. Quantitative PCR clearly showed significant up-regulation of all five transcripts in iPS-CMs grown on stiff gels therefore strongly implicating that all 5 transcripts are potential indicators of mechanical stress exerted in cardiomyocytes exposed to fibrosis-like matrix stiffness (Fig. 4).

A newly identified transcript with increased expression in iPS-CMs on stiff gels is Igf2. iPS-CMs were cultured on soft, medium and stiff gels for 4 weeks and labeled with antibodies against the IGF2 protein (Fig. 5). The mean cell fluorescence (soft: n = 14, medium: n = 22, stiff: n = 27) was measured after normalization to the

Table 1
Absolute expression values of selected transcripts on soft, medium and stiff hydrogels as well as on plastic.

Probe set ID	Gene Symbol	Expression normal scale			
		soft	medium	stiff	plastic
1417945_at	Pou5f1	7,3	9,3	8,9	9,1
1418726_a_at	Tnnt2	10142,3	9606,5	10703,5	9480,2
1416967_at	Sox2	3,6	4,2	4,1	3,6
1419944_at	Ccnb1	8,8	9,8	8,3	7,9
1449177_at	Ccna1	6,3	6,3	6,1	6,9
1415927_at	Actc1	13747,7	13977,3	13991,9	14117,5

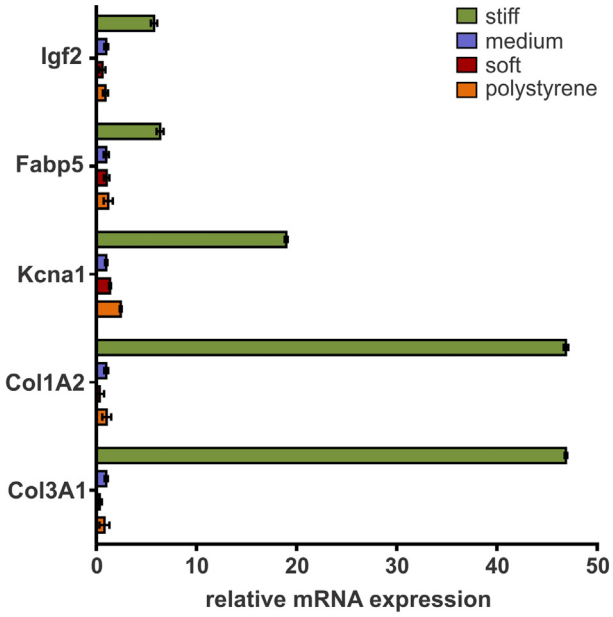

Fig. 4. Quantitative polymerase chain reaction. The expression of a selection of up-regulated transcripts was verified by real-time PCR.

background (Fig. 6, $^{***}P < 0.001$). Our results clearly demonstrate a marked increase in Igf2 expression in iPS-CMs on stiff gels as predicted by the gene array and quantitative PCR analysis. The presence of Igf2 in perinuclear vesicles points to an intact recycling mechanism that is known to internalize receptor-bound Igf2 from the cell membrane.

3.4. Comparison of fibronectin and laminin as ECM ligand

It might be argued that fibronectin itself induces ECM synthesis in plated cells. To address this question iPS-CMs were cultured for four weeks on medium gels coated with fibronectin or laminin (N = 3 for fibronectin, N = 2 for laminin). RNA was isolated and the transcription profile was analyzed on Clariom S gene arrays. Among > 22.000 detected transcripts only natriuretic protein type B (NPPB) was found more than 3-fold upregulated (3.1-fold) in iPS-CMs cultured on fibronectin (Supplementary Table 5). No other annotated transcript showed above 3-fold expression difference between the fibronectin and the laminin group.

We made further use of the dataset to compare the expression of myosin heavy chain isoform alpha (MYH6) and myosin heavy chain isoform beta (MYH7) at transcript level in order to obtain information on the differentiation status of the cells. It has previously been described (in rats) that MYH7 is the predominant iso-

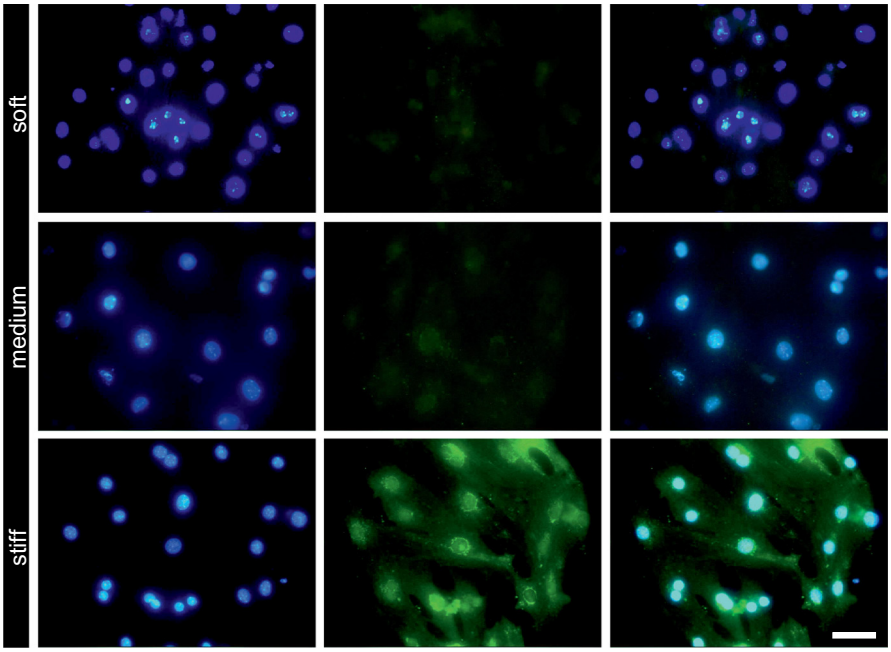

Fig. 5. Immunological detection of IGF2. Immunocytochemical staining displays the expression of IGF2 (green) on soft, medium and stiff hydrogels. Nuclei were stained by Hoechst dye (blue). Scale bar: 20 μm. (For interpretation of the references to color in this figure legend, the reader is referred to the web version of this article.)

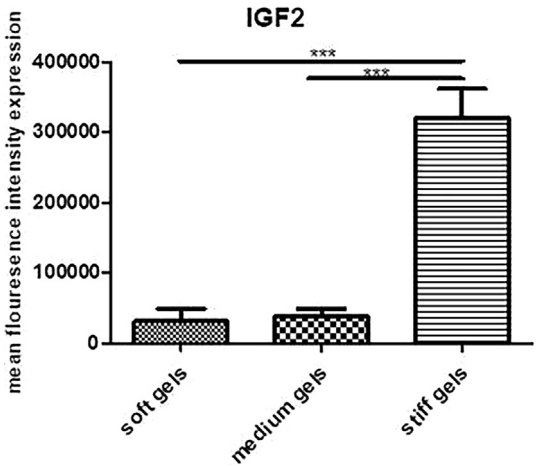

Fig. 6. Mean fluorescence of anti-Igf2 stained iPS-CMs grown for 4 weeks on soft, medium and stiff hydrogels. Data is presented as mean ± SEM. ***$P < 0.001$.

form in the embryonic rodent heart [34]. By comparing the expression values we found that the adult form MYH6 to be 25-fold higher expressed than MYH7, corresponding to an above 3 week old animal in the work of Lompré and colleagues [34].

3.5. Scanning electron microscopic analysis of cardiomyocytes reveals sarcomere structures and ECM deposition

In order to reveal cellular ultrastructure and detect potential matrix depositions, scanning electron microscopy was performed. iPS-CMs cultivated on hydrogels were well attached and spread on the surface of all gels (Fig. 7A, C, E). Cells were covered with singular short microvilli and some vesicles were recognized on the cell surface studied with secondary electron mode (Fig. 7A, C, E, marked with dashed-line circles). Using backscattered electron mode, we observed internal cell structures and detected in all studied groups typical and well-recognizable sarcomere structures, parallel-oriented in soft and medium hydrogels (Fig. 7B, D, Z-discs, marked with dashed-line rectangle) and disoriented on stiff substrate (Fig. 7F, Z-discs, marked with dashed-line rectangle). These findings strongly correlate with the alpha-actinin immunocytochemistry staining shown previously in Fig. 2. Examining iPS-CMs cultivated on stiff hydrogels, we have revealed a network of single fine fibers of approximately 100–150 nm in diameter located on the cell surface (Fig. 7G, arrows) and on the substrate (Fig. 7H, arrows). In addition, numerous small particles (Fig. 7G, H, asterisks) and shapeless or fibrillar clot formations (Fig. 7H, black and white double asterisks) were found coinciding with the fibers size and position. The fine fibers, small particles and clots, correspond to the mixing of filamentous and jellied extracellular matrix proteins together with proteoglycans secreted by the cardiomyocytes.

3.6. Effect of matrix elasticity on primary cardiac fibroblasts in comparison to iPS-CMs

We have observed increased expression of a variety of compounds of the cardiac ECM by iPS-CMs on stiff hydrogels. To rule out that our results are caused by contaminating fibroblasts that become activated by stiff matrix environments to produce collagens among other matrix proteins, an experiment with CFs was conducted. Primary CFs were freshly isolated from adult murine hearts and transferred to soft, medium and stiff hydrogels as well as polystyrene tissue culture plates. Samples were cultured for 4 weeks and mRNA was harvested from the cell preparations. Transcription profiling was performed and > 2-fold up- and down-regulated transcripts were compared to the results generated with iPS-CMs. Cellnet analysis identified cells as fibroblasts based on their transcriptomic profile (Supplementary Fig. 4). Results were analyzed in form of VENN diagrams (Fig. 8). Only 1 up-regulated and 2 down-regulated transcripts found in CFs on polystyrene were also found in iPS-CMs cultured for 4 weeks on stiff hydrogels. No overlap was found in up-regulated transcripts from CFs and iPS-CMs on soft hydrogel, while 3 transcripts were downregulated in both cell types. Finally, on stiff hydrogels, out of 572 transcripts that were upregulated in CFs,only 41 were also found to be upregulated in iPS-CMs. Remarkably, collagens I and III were not found among the upregulated transcripts in CFs (see Supplementary Table 4 for all results with CFs). The analysis of down-regulated transcripts revealed even more pronounced differences between the cell types with 404 transcripts that were specifically down-regulated in CFs and only 11 transcripts down-regulated both in CFs and iPS-CMs.

4. Discussion

To date, it has been generally accepted that ECM is produced exclusively by CFs in healthy conditions and by myofibroblasts and other inflammatory cells upon changes in mechanical, chemical or electrical signals in the myocardium. Here, we provide direct evidence that cardiomyocytes contribute to the formation of ECM upon exposure to stiff matrix conditions. Our results suggest that cardiomyocytes play a pivotal role in the pathological remodelling of the heart with potential implications for the understanding of cardiac fibrosis. To our best knowledge, this is the first report to combine *in vitro* engineered matrices exhibiting defined mechanical properties with highly purified iPS cell-derived cardiomyocytes to predict the transcriptomic changes occurring in cardiomyocytes in fibrotic tissues *in vivo*.

We observed arrhythmic beating in monocultures of iPS-CMs grown on stiff hydrogels. This observation is in line with previous reports in primary rat neonatal cardiomyocytes demonstrating arrhythmic contractions on 144 kPa stiff substrates [5,15]. An intriguing explanation could be the altered expression of Fgf11 and the significantly increased expression of the neuronal potassium channel (Kcna1), both pointing to a disturbed balancing of ion fluxes over the cell membrane. The role of Fgf11 in cardiomyocytes is related to regulation of voltage-gated sodium and calcium channels [35,36] and is also known to be a potential player in the pathophysiology of arrhythmias [36].

Our results demonstrating the presence of the voltage rectifier potassium channel Kv1.1 in cardiomyocytes cultured on fibrotic stiffness matrix lends further credence to the findings by Glasscock et al., who previously described an expression of the neuronal Kv1.1 channel in cardiomyocytes from atrial tissue of patients suffering from chronic atrial fibrillation and associated atrial fibrosis [37]. Whether the overexpression of the Kv1.1 potassium channels under fibrotic conditions plays a role in the increased susceptibility for arrhythmias in patients with fibrotic heart diseases however remains to be deciphered. No arrhythmia has been observed on matrices with native myocardium elasticity and it will be interesting to further investigate the clinical implications of our findings on the effect of anti-arrhythmic drugs on the disturbed synchronicity of cardiomyocytes grown on hydrogels with fibrotic properties.

Interestingly, the contractile function of iPS-CMs on conventional polystyrene substrates was severely disturbed even when compared to iPS-CMs on stiff PAA hydrogels. Data presented in previous studies in the field of cardiac cell replacement therapy suggests disassembly of sarcomeric structures in iPS-CMs grown on conventional substrates [11,38]. This finding is further under-

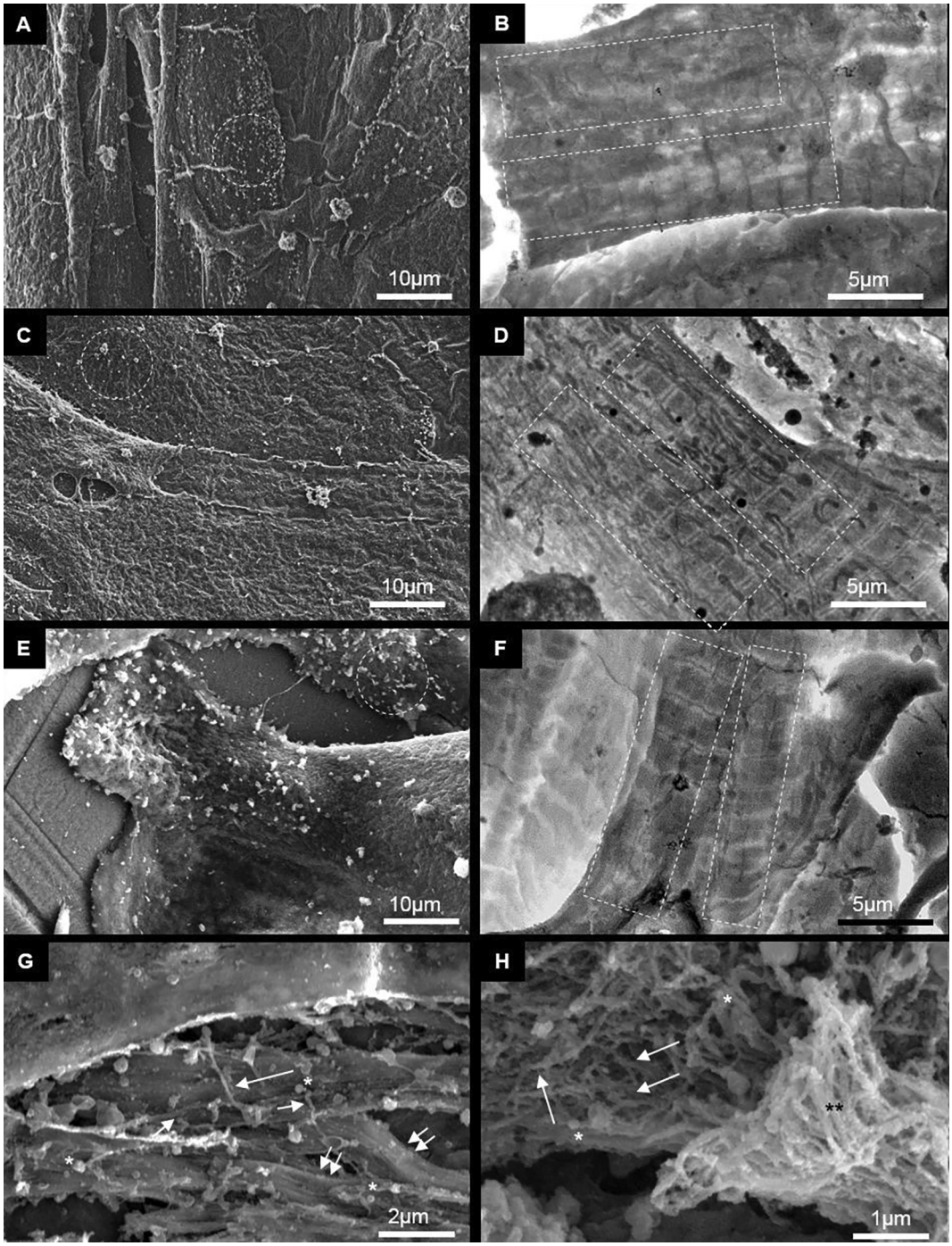

Fig. 7. Scanning electron microscopic images of iPS-CMs, seeded on soft (A,B), medium (C,D) and stiff (E-H) hydrogels. A, C, E, G and H are secondary electron images; B, D and F performed in backscattered electron mode of SEM. Z-discs are marked with dashed-line rectangles. Small microvilli and vesicles are marked with dashed-line circles. Single fine fibers of extracellular matrix are marked by arrows and bundles of matrix fibers are marked by double arrows. Asterisks indicate small particles and double asterisks label shapeless (white) and fibrillar (black) clots of matrix.

lined by the upregulation of stress-associated proteins and disturbed expression of transcripts involved in cellular metabolism. Based on these findings, it should be carefully considered whether culturing of iPS-CMs on conventional plastic surfaces is the optimal approach for providing healthy cardiomyocytes for sensitive applications such as regenerative medicine and *in vitro* pharmacological and toxicological assays.

Alteration of collagen fibrils composition, synthesis and degradation together with enhanced crosslinking forms the hallmark of cardiac stiffness and fibrosis [39]. Our data from pure iPS-CMs revealed strong up-regulation of Col1a1 and Col3a1which are near identical levels to those found by Qiu and colleagues [33] in primary progenitor cardiac cells cultured on stiff PDMS matrices. In our study, other collagen subtypes were also found specifically up-regulated in iPS-CMs cultured on fibrotic-stiffness like hydrogels (Col1a2, Col5a2, Col6a3 and Col8a2) pointing to a cell type specific pattern. Moreover, in line with our findings of increased expression of collagen III are the results from Weber and colleagues in a non-human primate model of hypertension-induced left ventricular hypertrophy. They showed fibrotic tissue alter-

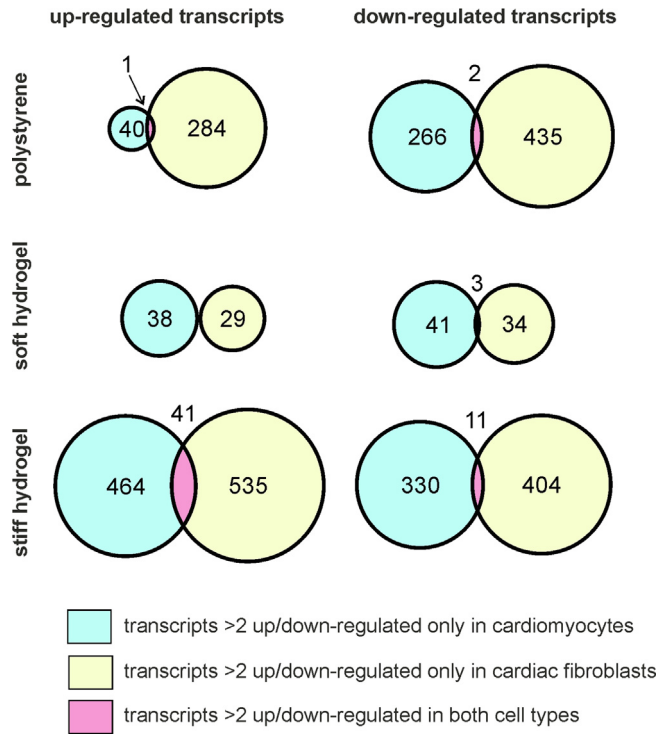

Fig. 8. Venn diagram comparing up- and down-regulated transcripts in cardiac fibroblasts and iPS-CMs on polystyrene, soft and stiff hydrogel compared to medium hydrogel. Numbers indicate the number of more, respectively, <2-fold up- and down-regulated transcripts in primary cardiac fibroblasts and iPS-CMs.

ations four weeks after experimental onset of hypertrophy, hence suggesting a hypertrophy-induced fibrosis [40].

In two different murine models of left ventricular remodelling (aortic banding [41] and right ventricular pressure overload following pulmonary artery banding [42]), lumican and decorin levels were shown to be increased in the affected hearts. Both proteoglycans - known to play a role in collagen fibrils stability and to be exclusively produced by cardiac fibroblasts [43] – were as well among the highly up-regulated genes found in iPS-CMs cultured on stiff matrix in our study. Further modifiers of the extracellular matrix were found to be upregulated in iPS-CMs on stiff hydrogel matrices, Mmp2, Mmp14, Timp2, Timp3, Spp1, and Tnc among them. Collectively, these results indicate that cardiomyocytes can produce both ECM proteins and their modulators MMPs and TIMPs, hence further supporting the hypothesis that cardiomyocytes contribute to ECM remodeling and cardiac fibrosis in a coordinated fashion. We have conclusively shown that collagen I is actively secreted by cardiomyocytes under fibrotic matrix conditions. This is demonstrated through the strong upregulation of the collagen I transcript (among other collagens) in our *in vitro* assay. Moreover, fibrillar matrix proteins were clearly identified on the cell surface as well as on the stiff hydrogels by electron microscopy. A secretion of collagens by cardiomyocytes into the extracellular space including the intercalated disk could be of large clinical impact, because impairment of electrical conductance is a hallmark of heart failure.

Our data not only demonstrate that transcripts previously described in cardiac fibrosis and attributed mainly to fibroblasts and myofibroblasts are strongly induced in cardiomyocytes under adverse matrix conditions but also point to novel candidates of potential interest. Recently, Shen and colleagues reported that IGF2 plays a role in embryonic ventricular wall development and that it is primarily expressed in the epicardium [44]. Nevertheless, our study demonstrates for the first time that Igf2 could be re-expressed by cardiomyocytes facing fibrotic-like conditions thus suggesting a new role for Igf2 in cardiac hypertrophy, remodelling and fibrosis.

As a limitation of our study appears the choice of elastic moduli used for the experiments. Previously reported Young's moduli were used as references to generate hydrogels matching the putative elastic modulus of embryonic, adult and fibrotic cardiac tissue. However, other groups have reported varying reference values. Berry and colleagues reported a value of 18 ± 2 kPa for healthy rat myocardium and 55 ± 15 kPa for fibrotic tissue [45]. Based on these values 30 kPa stiffness as used in our study could be more rigid than non-fibrotic myocardium. There is indeed a hint that points in this direction: We could observe sarcomere fracture in individual cells (shown in supplementary Fig. 1). Even though we did not analyze enough material to analyze this observation further the finding is in line with a report of Ribeiro and colleagues demonstrating the occurrence of sarcomere fracture in cardiomyocytes on hydrogels with 35 kPa stiffness [46].

Another limitation in the comparison of cells cultured on polystyrene and polyacrylamide are differences beside the elastic modulus of the substrates. On polystyrene protein ligands are passively absorbed to a plane surface. In contrast the surface of polyacrylamide is structured and proteins are immobilized by reaction of primary amines present in the side chain of the amino acid lysine and the reactive ester group of the DAH molecule. It cannot be excluded that differences in the surface structure of the polymer and potential conformational differences of the protein ligands affected the behavior of the cultured cardiomyocytes.

Taken together, our data clearly show that genes known to be up-regulated in cardiac fibroblasts and myofibroblasts during pathological cardiac remodelling are also up-regulated at the level of the cardiomyocyte cell. This suggests a potential role for cardiomyocytes in the detrimental process of ECM remodeling during fibrosis leading to heart failure. It becomes obvious that our refined *in vitro* approach has allowed us to identify the transcriptional signatures known to have a pivotal role in cardiac fibrosis *in vivo*. Furthermore, based on this concept, it can be concluded that newly up- and down-regulated transcripts identified here, have a strong potential to play a key role in cardiac fibrosis *in vivo*. In conclusion, we have not only shown that cardiomyocytes secrete ECM, but also provided a new reproducible approach to further study the underlying complex molecular and cellular mechanisms of cardiac fibrosis. Whether the fibrotic response of cardiomyocytes is reversible and whether the mechanisms controlling the detected cardiomyocyte maladaptation could be targeted for regenerative therapy, remains to be elucidated.

Acknowledgements

We thank Anette Peffekoven, Annette Köster, Margit Henry, Norbert Pütz and Tamara Rotsteyn for excellent technical assistance. Imaging was performed at the CECAD facilities of the medical faculty, University of Cologne. Gene arrays were analyzed at the transcriptomics facility at CMMC, Cologne.

Funding Sources

This work was supported by the German Federal Ministry of Education and Research (project 031B0050) and the Elisabeth-und-Rudolf-Hirsch-Stiftung. Nelly Mikhael was supported by a GERLS long-term scholarship from the German Academic Exchange Service (DAAD).

Appendix A. Supplementary data

Supplementary data to this article can be found online at https://doi.org/10.1016/j.actbio.2019.03.017.

References

[1] I. Manabe, T. Shindo, R. Nagai, Gene expression in fibroblasts and fibrosis: involvement in cardiac hypertrophy, Circ. Res. 91 (12) (2002) 1103–1113.
[2] S.L. Bowers, I. Banerjee, T.A. Baudino, The extracellular matrix: at the center of it all, J. Mol. Cell. Cardiol. 48 (3) (2010) 474–482.
[3] R.R. Chaturvedi, T. Herron, R. Simmons, D. Shore, P. Kumar, B. Sethia, F. Chua, E. Vassiliadis, J.C. Kentish, Passive stiffness of myocardium from congenital heart disease and implications for diastole, Circulation 121 (8) (2010) 979–988.
[4] P. Kong, P. Christia, N.G. Frangogiannis, The pathogenesis of cardiac fibrosis, Cell. Mol. Life Sci. 71 (4) (2014) 549–574.
[5] A.J. Engler, C. Carag-Krieger, C.P. Johnson, M. Raab, H.Y. Tang, D.W. Speicher, J. W. Sanger, J.M. Sanger, D.E. Discher, Embryonic cardiomyocytes beat best on a matrix with heart-like elasticity: scar-like rigidity inhibits beating, J. Cell Sci. 121 (Pt 22) (2008) 3794–3802.
[6] K. Schram, S. De Girolamo, S. Madani, D. Munoz, F. Thong, G. Sweeney, Leptin regulates MMP-2, TIMP-1 and collagen synthesis via p38 MAPK in HL-1 murine cardiomyocytes, Cell. Mol. Biol. Lett. 15 (4) (2010) 551–563.
[7] S.L. Schor, A.M. Schor, Phenotypic and genetic alterations in mammary stroma: implications for tumour progression, Breast Cancer Res. 3 (6) (2001) 373–379.
[8] C. Mauritz, K. Schwanke, M. Reppel, S. Neef, K. Katsirntaki, L.S. Maier, F. Nguemo, S. Menke, M. Haustein, J. Hescheler, G. Hasenfuss, U. Martin, Generation of functional murine cardiac myocytes from induced pluripotent stem cells, Circulation 118 (5) (2008) 507–517.
[9] K. Pfannkuche, H. Liang, T. Hannes, J. Xi, A. Fatima, F. Nguemo, M. Matzkies, M. Wernig, R. Jaenisch, F. Pillekamp, M. Halbach, H. Schunkert, T. Saric, J. Hescheler, M. Reppel, Cardiac myocytes derived from murine reprogrammed fibroblasts: intact hormonal regulation, cardiac ion channel expression and development of contractility, Cell. Physiol. Biochem. 24 (1–2) (2009) 73–86.
[10] M.G. Klug, M.H. Soonpaa, G.Y. Koh, L.J. Field, Genetically selected cardiomyocytes from differentiating embronic stem cells form stable intracardiac grafts, J. Clin. Invest. 98 (1) (1996) 216–224.
[11] C.O. Heras-Bautista, A. Katsen-Globa, N.E. Schloerer, S. Dieluweit, O.M. Abd El Aziz, G. Peinkofer, W.A. Attia, M. Khalil, K. Brockmeier, J. Hescheler, K. Pfannkuche, The influence of physiological matrix conditions on permanent culture of induced pluripotent stem cell-derived cardiomyocytes, Biomaterials 35 (26) (2014) 7374–7385.
[12] W.L. Chen, M. Likhitpanichkul, A. Ho, C.A. Simmons, Integration of statistical modeling and high-content microscopy to systematically investigate cell-substrate interactions, Biomaterials 31 (9) (2010) 2489–2497.
[13] M.L. McCain, H. Yuan, F.S. Pasqualini, P.H. Campbell, K.K. Parker, Matrix elasticity regulates the optimal cardiac myocyte shape for contractility, Am. J. Physiol. Heart Circ. Physiol. 306 (11) (2014) H1525–H1539.
[14] A.G. Rodriguez, S.J. Han, M. Regnier, N.J. Sniadecki, Substrate stiffness increases twitch power of neonatal cardiomyocytes in correlation with changes in myofibril structure and intracellular calcium, Biophys. J. 101 (10) (2011) 2455–2464.
[15] B. Bhana, R.K. Iyer, W.L. Chen, R. Zhao, K.L. Sider, M. Likhitpanichkul, C.A. Simmons, M. Radisic, Influence of substrate stiffness on the phenotype of heart cells, Biotechnol. Bioeng. 105 (6) (2010) 1148–1160.
[16] P. Pandey, W. Hawkes, J. Hu, W.V. Megone, J. Gautrot, N. Anilkumar, M. Zhang, L. Hirvonen, S. Cox, E. Ehler, J. Hone, M. Sheetz, T. Iskratsch, Cardiomyocytes sense matrix rigidity through a combination of muscle and non-muscle myosin contractions, Dev. Cell 45 (5) (2018) 661.
[17] Y. Shiba, T. Gomibuchi, T. Seto, Y. Wada, H. Ichimura, Y. Tanaka, T. Ogasawara, K. Okada, N. Shiba, K. Sakamoto, D. Ido, T. Shiina, M. Ohkura, J. Nakai, N. Uno, Y. Kazuki, M. Oshimura, I. Minami, U. Ikeda, Allogeneic transplantation of iPS cell-derived cardiomyocytes regenerates primate hearts, Nature 538 (7625) (2016) 388–391.
[18] Y.W. Liu, B. Chen, X. Yang, J.A. Fugate, F.A. Kalucki, A. Futakuchi-Tsuchida, L. Couture, K.W. Vogel, C.A. Astley, A. Baldessari, J. Ogle, C.W. Don, Z.L. Steinberg, S.P. Seslar, S.A. Tuck, H. Tsuchida, A.V. Naumova, S.K. Dupras, M.S. Lyu, J. Lee, D. W. Hailey, H. Reinecke, L. Pabon, B.H. Fryer, W.R. MacLellan, R.S. Thies, C.E. Murry, Human embryonic stem cell-derived cardiomyocytes restore function in infarcted hearts of non-human primates, Nat. Biotechnol. 36 (7) (2018) 597–605.
[19] W. Hiesinger, M.J. Brukman, R.C. McCormick, J.R. Fitzpatrick III, J.R. Frederick, E. C. Yang, J.R. Muenzer, N.A. Marotta, M.F. Berry, P. Atluri, Y.J. Woo, Myocardial tissue elastic properties determined by atomic force microscopy after stromal cell-derived factor 1alpha angiogenic therapy for acute myocardial infarction in a murine model, J. Thorac. Cardiovasc. Surg. 143 (4) (2012) 962–966.
[20] D.K. Bogen, A. Needleman, T.A. McMahon, An analysis of myocardial infarction. The effect of regional changes in contractility, Circ. Res. 55 (6) (1984) 805–815.
[21] J.G. Jacot, J.C. Martin, D.L. Hunt, Mechanobiology of cardiomyocyte development, J. Biomech. 43 (1) (2010) 93–98.
[22] J.L. Hutter, Bechhoefer., J, Calibration of atomic-force microscope tips, Rev. Sci. Instrum. 64 (1993) 1868–1873.
[23] H. Hertz, Über die Berührung fester elastischer Körper, Journal für die reine und angewandte Mathematik 92 (1882) 156–171.
[24] I.N. Sneddon, The relation between load and penetration in the axisymmetric boussinesq problem for a punch of arbitrary profile, Int. J. Eng. Sci. 3 (1965) 47–57.
[25] M. Radmacher, M. Fritz, P.K. Hansma, Imaging soft samples with the atomic force microscope: gelatin in water and propanol, Biophys. J . 69 (1) (1995) 264–270.
[26] A.L. Weisenhorn, M. Khorsandi, S. Kasas, V. Gotzos, H.J. Butt, Deformation and height anomaly of soft surfaces studied with an AFM, Nanotechnology 106 (1993).
[27] J. Semmler, M. Lehmann, K. Pfannkuche, M. Reppel, J. Hescheler, F. Nguemo, Functional expression and regulation of hyperpolarization-activated cyclic nucleotide-gated channels (HCN) in mouse iPS cell-derived cardiomyocytes after UTF1 -neo selection, Cell. Physiol. Biochem. 34 (4) (2014) 1199–1215.
[28] K. Pfannkuche, S. Neuss, F. Pillekamp, L.P. Frenzel, W. Attia, T. Hannes, J. Salber, M. Hoss, M. Zenke, B.K. Fleischmann, J. Hescheler, T. Saric, Fibroblasts facilitate the engraftment of embryonic stem cell-derived cardiomyocytes on three-dimensional collagen matrices and aggregation in hanging drops, Stem Cells Dev. 19 (10) (2010) 1589–1599.
[29] K. Meganathan, S. Jagtap, S.P. Srinivasan, V. Wagh, J. Hescheler, J. Hengstler, M. Leist, A. Sachinidis, Neuronal developmental gene and miRNA signatures induced by histone deacetylase inhibitors in human embryonic stem cells, Cell Death Dis. 6 (2015) e1756.
[30] P. Cahan, H. Li, S.A. Morris, D.R. Lummertz, G.Q. Daley, J.J. Collins, Cell Net: network biology applied to stem cell engineering, Cell 158 (4) (2014) 903–915.
[31] A.D. Katsen, B. Vollmar, P. Mestres-Ventura, M.D. Menger, Cell surface and nuclear changes during TNF-alpha-induced apoptosis in WEHI 164 murine fibrosarcoma cells. A correlative light, scanning, and transmission electron microscopical study, Virchows Arch 433 (1) (1998) 75–83.
[32] E. Kolossov, T. Bostani, W. Roell, M. Breitbach, F. Pillekamp, J.M. Nygren, P. Sasse, O. Rubenchik, J.W. Fries, D. Wenzel, C. Geisen, Y. Xia, Z. Lu, Y. Duan, R. Kettenhofen, S. Jovinge, W. Bloch, H. Bohlen, A. Welz, J. Hescheler, S.E. Jacobsen, B.K. Fleischmann, Engraftment of engineered ES cell-derived cardiomyocytes but not BM cells restores contractile function to the infarcted myocardium, J. Exp. Med. 203 (10) (2006) 2315–2327.
[33] Y. Qiu, A.F. Bayomy, M.V. Gomez, M. Bauer, P. Du, Y. Yang, X. Zhang, R. Liao, A role for matrix stiffness in the regulation of cardiac side population cell function, Am. J. Physiol Heart Circ. Physiol 308 (9) (2015) H990–H997.
[34] A.M. Lompre, B. Nadal-Ginard, V. Mahdavi, Expression of the cardiac ventricular alpha- and beta-myosin heavy chain genes is developmentally and hormonally regulated, J. Biol. Chem. 259 (10) (1984) 6437–6446.
[35] C. Wang, C. Wang, E.G. Hoch, G.S. Pitt, Identification of novel interaction sites that determine specificity between fibroblast growth factor homologous factors and voltage-gated sodium channels, J. Biol. Chem. 286 (27) (2011) 24253–24263.
[36] J.A. Hennessey, E.Q. Wei, G.S. Pitt, Fibroblast growth factor homologous factors modulate cardiac calcium channels, Circ. Res. 113 (4) (2013) 381–388.
[37] E. Glasscock, N. Voigt, M.D. McCauley, Q. Sun, N. Li, D.Y. Chiang, X.B. Zhou, C.E. Molina, D. Thomas, C. Schmidt, D.G. Skapura, J.L. Noebels, D. Dobrev, X.H. Wehrens, Expression and function of Kv1.1 potassium channels in human atria from patients with atrial fibrillation, Basic Res. Cardiol. 110(5) (2015) 505.
[38] L. Ye, Y.H. Chang, Q. Xiong, P. Zhang, L. Zhang, P. Somasundaram, M. Lepley, C. Swingen, L. Su, J.S. Wendel, J. Guo, A. Jang, D. Rosenbush, L. Greder, J.R. Dutton, J. Zhang, T.J. Kamp, D.S. Kaufman, Y. Ge, J. Zhang, Cardiac repair in a porcine model of acute myocardial infarction with human induced pluripotent stem cell-derived cardiovascular cells, Cell Stem Cell 15 (6) (2014) 750–761.
[39] B.C. Berk, K. Fujiwara, S. Lehoux, ECM remodeling in hypertensive heart disease, J. Clinical Investigation 117 (3) (2007) 568–575.
[40] K.T. Weber, J.S. Janicki, S.G. Shroff, R. Pick, R.M. Chen, R.I. Bashey, Collagen remodeling of the pressure-overloaded, hypertrophied nonhuman primate myocardium, Circ. Res. 62 (4) (1988) 757–765.
[41] K.V. Engebretsen, A. Waehre, J.L. Bjornstad, B. Skrbic, I. Sjaastad, D. Behmen, H. S. Marstein, A. Yndestad, P. Aukrust, G. Christensen, T. Tonnessen, Decorin, lumican, and their GAG chain-synthesizing enzymes are regulated in myocardial remodeling and reverse remodeling in the mouse, J. Appl. Physiol. 114 (8) (2013) 988–997.
[42] A. Waehre, M. Vistnes, I. Sjaastad, S. Nygard, C. Husberg, I.G. Lunde, P. Aukrust, A. Yndestad, L.E. Vinge, D. Behmen, C. Neukamm, H. Brun, E. Thaulow, G. Christensen, Chemokines regulate small leucine-rich proteoglycans in the extracellular matrix of the pressure-overloaded right ventricle, J. Appl. Physiol. (1985) 112 (8) (2012) 1372–1382.
[43] L.E. Dupuis, M.G. Berger, S. Feldman, L. Doucette, V. Fowlkes, S. Chakravarti, S. Thibaudeau, N.E. Alcala, A.D. Bradshaw, C.B. Kern, Lumican deficiency results in cardiomyocyte hypertrophy with altered collagen assembly, J. Mol. Cell. Cardiol. 84 (2015) 70–80.
[44] H. Shen, S. Cavallero, K.D. Estrada, I. Sandovici, S.R. Kumar, T. Makita, C.L. Lien, M. Constancia, H.M. Sucov, Extracardiac control of embryonic cardiomyocyte proliferation and ventricular wall expansion, Cardiovasc. Res. 105 (3) (2015) 271–278.
[45] M.F. Berry, A.J. Engler, Y.J. Woo, T.J. Pirolli, L.T. Bish, V. Jayasankar, K.J. Morine, T.J. Gardner, D.E. Discher, H.L. Sweeney, Mesenchymal stem cell injection after myocardial infarction improves myocardial compliance, Am. J. Physiol. Heart Circ. Physiol. 290 (6) (2006) H2196–H2203.
[46] A.J. Ribeiro, Y.S. Ang, J.D. Fu, R.N. Rivas, T.M. Mohamed, G.C. Higgs, D. Srivastava, B.L. Pruitt, Contractility of single cardiomyocytes differentiated from pluripotent stem cells depends on physiological shape and substrate stiffness, Proc. Natl. Acad. Sci. USA 112 (41) (2015) 12705–12710.